

## Three-Dimensional Transition in the Wake of an Ellipse

J. S. Leontini<sup>1</sup>, D. Lo Jacono<sup>2,3</sup> and M. C. Thompson<sup>2</sup>

<sup>1</sup>Department of Mechanical and Product Design Engineering  
Swinburne University of Technology, John St Hawthorn, Victoria 3162, Australia

<sup>2</sup>Fluids Laboratory for Aeronautical and Industrial Research (FLAIR), Department of Mechanical And Aerospace Engineering

Monash University, Wellington Rd Clayton, Victoria 3800, Australia

<sup>3</sup>Université de Toulouse; INP; IMFT (Institut de Mécanique des Fluides de Toulouse)  
Allée Camille Soula, F-31400 Toulouse, France

### Abstract

The transition to three-dimensional flow from the nominally two-dimensional Kármán vortex street in the wake of bluff bodies is a problem of fundamental importance as it marks the first step on the path towards fully developed turbulence. Here, this transition is studied in the wake of an elliptical cross-section using Floquet stability analysis. A number of modes of instability are identified as a function of the aspect ratio of the ellipse. Three-dimensional simulations confirm the importance of the identified instability modes.

### Introduction

This paper reports on the results of a study of the linear stability of the Kármán vortex street in the wake of an elliptical cross-section. The aim is to identify the instability modes that cause the wake to cease being uniform in the spanwise direction (two-dimensional) and to become three-dimensional.

The flow is governed by two parameters: the Reynolds number  $Re = UD/\nu$ , where  $U$  is the freestream velocity,  $D$  is the width of the cross-section across the flow, and  $\nu$  is the kinematic viscosity; and the elliptical cross-section aspect ratio  $\Gamma = L/D$ , where  $L$  is the length of the body in the flow direction. When  $\Gamma = 1$ , the body is a circular cylinder. As  $\Gamma$  is increased beyond  $\Gamma > 1$ , the body becomes a streamlined ellipse. Here, flow for bodies  $1 \leq \Gamma \leq 2.4$  are studied.

Two-dimensional direct numerical simulations have been performed for a series of values of  $\Gamma$  and  $Re$ . The stability of these base flows has then been established using Floquet stability analysis. Five instability modes have been identified, and their dependence on  $\Gamma$  ascertained. Of these five modes, two are only found above a certain value of  $\Gamma$ , meaning they do not occur in the wake of a circular cylinder. Fully three-dimensional direct numerical simulations have also been performed, confirming the existence of the saturated state of these two new modes.

### Methodology

#### Floquet Stability Analysis

In general, Floquet stability analysis is a technique to ascertain the stability of periodic solutions. Here, the periodic solution is the two-dimensional Kármán vortex street. To assess the stability, first linear equations are formed that govern the evolution of a perturbation to the periodic solution. The perturbation equations are integrated forward in time one period, and the size of the perturbation is compared to its size one period prior. This process is repeated over many iterations. The ratio of the size of the perturbation at the current period to that at the previous pe-

riod is known as the Floquet multiplier,  $\mu_f$ . If the perturbation has grown over one period,  $|\mu_f| > 1$ , the original periodic solution is unstable; if the perturbation decays,  $|\mu_f| < 1$ , the original solution is stable. Note that  $\mu_f$  can be a complex number. If it is complex, this implies that the instability mode varies with a frequency that is incommensurate with the periodic base flow.

A further extension to the method is to decompose the perturbation into Fourier components in the spanwise direction. If this is done, it can be shown that the various Fourier modes decouple, and therefore the stability with respect to a perturbation of a specified spanwise wavelength  $\lambda$  can be ascertained. Therefore, the Floquet multiplier  $\mu_f$  is a function of the flow variables (in this case  $Re$  and  $\Gamma$ ) and the spanwise wavelength  $\lambda$ . A full explanation of this technique can be found [1].

Each instability mode will have a characteristic  $\lambda$ . At this  $\lambda$ ,  $\mu_f$  will be maximum for that mode. Therefore, when a point of marginal stability is found (a point in the  $\Gamma, Re$  plane where  $\mu_f = 1$ ), there is a corresponding value of  $\lambda$ . So, the main task of the analysis is to find the curves of marginal stability ( $\mu_f = 1$ ) in the  $\Gamma, Re$  plane for each mode and the wavelength  $\lambda$  at which this occurs.

#### Simulation Technique

Calculations were performed using a high-order spectral element method to solve the weak form of the incompressible Navier–Stokes equations for the base flows, and a linearized version of these same equations for the perturbation fields. Full details of the spectral-element method can be found [2]. Validation of the code employed here for the base flows and the stability analysis is given in a series of papers [3, 4, 5]. The generally complex Floquet multipliers (and the corresponding instability modes) were calculated using Arnoldi decomposition.

### Results and Discussion

#### Stability Analysis

Five distinct modes were found to become unstable in the wake of the ellipse, and representative images of each of them are shown in figure 1. The images show the spanwise perturbation vorticity as colour contours, and the base flow vorticity (the vortex street) as solid lines. The modes are shown in order of increasing characteristic wavelength, from top to bottom.

Three of the modes shown in figure 1 are known from studies of the circular cylinder, namely modes A, B, and QP. Mode A is thought to be due primarily to an elliptic instability of the wake vortices [6, 7], while mode B appears to be an instability of the shear layers in between the wake vortices. Mode QP is a quasiperiodic mode, meaning it has a frequency incommensu-

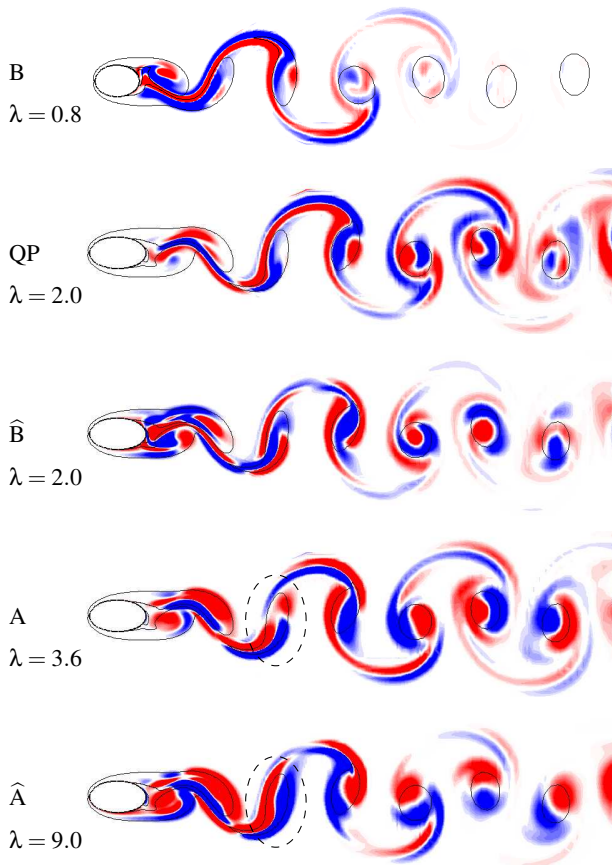


Figure 1: Images of the different modes at  $\Gamma = 1.8$  (except for mode B shown at  $\Gamma = 1.4$ ) shown in order of increasing characteristic wavelength. The red and blue contours represent spanwise perturbation vorticity over normalized levels of  $\pm 0.1$ . The solid lines show contours of the base flow vorticity at levels  $\pm 1$ . Mode  $\hat{B}$  has a distinct structure, but shares the same spatio-temporal symmetries as mode B. Mode  $\hat{A}$  has a similar structure to mode A in the two vortices closest to the body, but is distinct from the third vortex (circled with a dashed line) and further downstream.

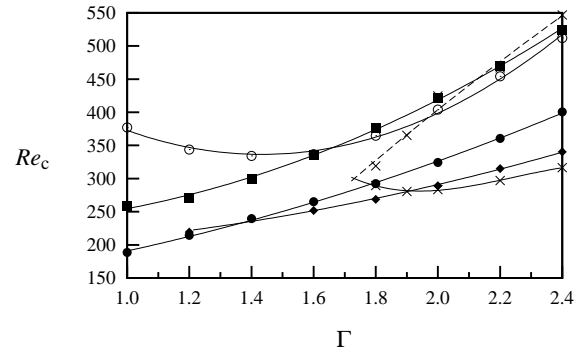


Figure 2:  $Re_c$ , the value of  $Re$  at marginal stability for all the modes as a function of  $\Gamma$ . Points are measured values for for mode A ( $\bullet$ ), mode B ( $\blacksquare$ ), mode QP ( $\circ$ ), mode  $\hat{A}$  ( $\blacklozenge$ ), mode  $\hat{B}$  ( $\times$ ). Lines are best fits to the measured values. The upper limit of instability for mode  $\hat{B}$  is marked with a dashed line as it is the result of extrapolation.

rate with the base flow, and therefore a complex Floquet multiplier [8].

Two new modes have been discovered that only occur for a range of  $\Gamma$ , and therefore do not occur in the circular cylinder wake. These are modes  $\hat{A}$  and  $\hat{B}$ . Mode  $\hat{A}$  has a structure very similar to mode A, until a few diameters downstream. In figure 1, the first vortex where a discernible difference between the structures of modes A and  $\hat{A}$  are circled with a dashed line. Mode  $\hat{B}$  has a spatio-temporal symmetry the same as mode B, however its spatial structure is quite distinct. It bears some resemblance to the mode named  $B'$  found in the wake of elliptical leading-edge plates [9].

The dependence of the critical Reynolds number  $Re_c$  on  $\Gamma$  for each of these five modes is shown in figure 2. Modes A and B are shown to be stabilized by increasing  $\Gamma$ , with  $Re_c$  increasing. Mode QP is initially destabilized for  $\Gamma < 1.2$ , but it stabilized with further increases in  $\Gamma$ . The instability scenario for  $\Gamma < 1.2$  is basically the same as for the circular cylinder; with increasing  $Re$ , mode A first becomes unstable, then mode B, then mode QP.

For  $\Gamma > 1.2$ , the transition scenario is different from the circular cylinder. Mode  $\hat{A}$  is resolved, and shown to be the first mode to become unstable with increasing  $Re$  for  $1.2 < \Gamma < 1.9$ . For  $\Gamma > 1.9$ , mode  $\hat{B}$  is the first to become unstable, followed by mode  $\hat{A}$ .

Other features of figure 2 are of note. First, mode  $\hat{B}$  is found to be unstable in a closed region of the parameter space, i.e. there is an upper limit to the range of  $Re$  where this mode is unstable. This upper limit is shown by the dashed line in figure 2. Second, mode  $\hat{A}$  appears to almost branch off from mode A around  $\Gamma = 1.2$ .

Further evidence of mode  $\hat{A}$  branching off from mode A is found by plotting the characteristic wavelength  $\lambda_c$  of modes A and  $\hat{A}$ , as found in figure 3. The figure shows that while the wavelength of mode A is weakly affected by increasing  $\Gamma$ , mode  $\hat{A}$  is strongly affected, with  $\lambda_c$  increasing almost linearly with  $\Gamma$ . At  $\Gamma = 1.2$ , the wavelengths of modes A and  $\hat{A}$  coincide, and for  $\Gamma < 1.2$  mode  $\hat{A}$  is not resolved. This indicates that the instability mechanism of mode  $\hat{A}$  is likely to rely on the structure of the wake close to the body in a similar way to mode A.

### Three-Dimensional Simulations

While the linear stability analysis can give some indication of

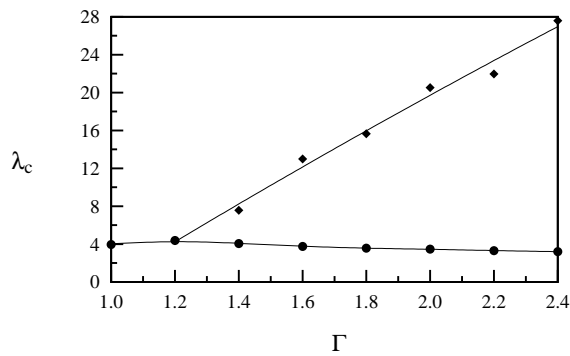


Figure 3: The wavelength at marginal stability as a function of  $\Gamma$  for modes A and  $\hat{A}$ . Mode  $\hat{A}$  appears to bifurcate from mode A around  $\Gamma = 1.2$ .

the parameter values for which the base flow is unstable, and the structure of the linear instability mode, it does not necessarily give a clear picture of the form of the flow beyond the bifurcation. This is because nonlinear effects are not captured in the stability analysis, which play a role in the development of the final fully saturated state. To capture this, fully three-dimensional direct numerical simulations are required.

The saturated state in the wake of a circular cylinder is well documented [10, 11], and depends primarily on modes A and B. However, the impact of the new modes  $\hat{A}$  and  $\hat{B}$  has not been previously reported.

Figure 4 presents results from simulations for  $\Gamma = 2$ , for  $Re = 300$  and  $Re = 350$ . In both cases, both modes  $\hat{A}$  and  $\hat{B}$  are predicted to be unstable according to figure 2.

For the simulations at  $Re = 300$  shown in figure 4a, the spanwise domain was restricted to  $9.6D$ . On this restricted domain, a clear wavelength of  $2.4D$  develops, attributable to mode  $\hat{B}$ . The three-dimensionality is relatively weak, restricted to a moderate waviness of the shear layer separating from the body and the vortex cores downstream.

For the simulations at  $Re = 350$  shown in figure 4b, the spanwise domain was extended to  $22D$ . In this case, a mode with a wavelength around  $7.5D$  becomes dominant in the saturated state. This is attributable to mode  $\hat{A}$ . This is despite mode  $\hat{B}$  becoming unstable at a lower  $Re$ . The flow state is quite complex, with an initial waviness of the separating shear layer, leading to a structure of essentially streamwise vortices developing further downstream. These streamwise structures appear to undergo a secondary instability around  $25D$  downstream, moving across the wake towards each other.

### Conclusions

Floquet stability analysis, and supporting three-dimensional direct numerical simulations, have been conducted of the wake of an elliptical cross-section. It has been shown that for small aspect ratios, the instability scenario is similar to that for a circular cylinder. However for larger aspect ratios, new modes of instability are resolved. These new modes have been shown to play a leading role in the fully saturated three-dimensional state of the flow.

### Acknowledgements

The authors acknowledge the financial support of the Australian Research Council through Discovery Project grant DP110102141, and the provision of computational resources and expertise of the Monash University e-research centre, and

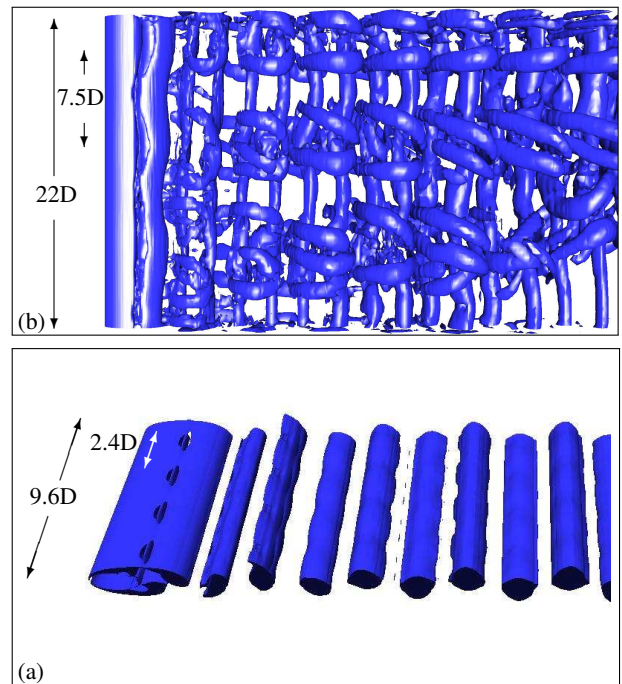


Figure 4: Visualization of the flow calculated from three-dimensional DNS at (a)  $\Gamma = 2$ ,  $Re = 300$ , mode  $\hat{B}$ , and (b)  $\Gamma = 2$ ,  $Re = 350$ , mode  $\hat{A}$ . Isosurfaces show the  $\lambda_2 = -0.001$  criterion [12]. The total length of the domain, and one wavelength of the dominant mode, are marked for both cases.

the National Computational Infrastructure (NCI).

### References

- [1] Barkley, C. and Henderson, R.D., Three-dimensional Floquet stability analysis of the wake of a circular cylinder, *J. Fluid Mech.*, **322**, 1996, 215–241
- [2] Karniadakis, G.Em. and Sherwin, S., *Spectral/hp element methods for computational fluid dynamics*, Oxford University, 2005.
- [3] Thompson, M.C., Hourigan, K., Cheung, A. and Leweke, T., Hydrodynamics of a particle impact on a wall, *App. Math. Model.*, **30(11)**, 2006, 1356–1369.
- [4] Leontini, J.S., Thompson, M.C. and Hourigan, K., Three-dimensional transition in the wake of a transversely oscillating cylinder, *J. Fluid Mech.*, **577**, 79–104
- [5] Rao, A., Leontini, J., Thompson, M.C. and Hourigan, K., Three-dimensionality in the wake of a rotating cylinder in a uniform flow, *J. Fluid Mech.*, **717**, 1–29
- [6] Leweke, T. and Williamson, C.H.K., Three-dimensional instabilities in wake transition, *Eur. J. Mech. B/Fluids*, **17(4)**, 571–586
- [7] Thompson, M.C., Leweke, T. and Williamson, C.H.K., The physical mechanism of transition in bluff body wakes, *J. Fluid Struct.*, **15**, 607–616
- [8] Blackburn, H.M., Marques, F. and Lopez, J.M., Symmetry breaking of two-dimensional time-periodic wakes, *J. Fluid Mech.*, **522**, 395–411

- [9] Ryan, K., Thompson, M.C. and Hourigan, K., Three-dimensional transition in the wake of bluff elongated cylinders, *J. Fluid Mech.*, **538**, 1–29
- [10] Williamson, C.H.K., The existence of two stages in the transition to three-dimensionality of a cylinder wake, *Phys. Fluids*, **31(11)**, 3165–3168
- [11] Thompson, M.C., Hourigan, K. and Sheridan, J. Three-dimensional instabilities in the wake of a circular cylinder, *Exp. Therm. Fluid Sci.*, **12**, 190–196
- [12] Jeong, J. and Hussain, F., On the identification of a vortex, *J. Fluid Mech.*, **285**, 69–94